Proceedings of the Technical Sessions, 39 (2023) 46-53
Institute of Physics, Sri Lanka

Fabrication of Copper (I) Oxide (Cu_2O) thin films on Transparent Conductive glass substrate

L W P M Madusanka[1], P K D D P Pitigala[1,2,*], C A N Fernando[1,3,4], P G D C K Karunarathna[3]

[1]*Department of Physics, Faculty of Applied Sciences, University of Sri Jayewardenepura*

[2]*Center for Advance Material Research, University of Sri Jayewardenepura*

[3]*Department of Nano Science Technology, Faculty of Technology, Wayamba University of Sri Lanka*

[4]*Department of Marine Engineering, Faculty of Engineering, Sir John Kotelawala Defense University, Sri Lanka*

[*]dpitigala@sjp.qc.lk

1. ABSTRACT

Copper (I) oxide (Cu_2O) is the most promising material recently used in solar cells, gas sensors, optical devices, and other areas. Most of the time, the Cu_2O thin film is fabricated on the opaque Cu substrate, which limits the absorption and photo-response of the film. As a result, the aim of this study is to develop a low-cost process to fabricate a Cu_2O thin film on a transparent conductive glass (ITO glass) substrate. The growth of Cu_2O thin film was carried out in two steps, with the first step being the electrodeposition of Copper (Cu) nanoparticles on ITO glass and the second stage involving the complete conversion of electroplated Cu on ITO glass to Cu_2O through low-temperature (< 95) thermal oxidation method. Morphological analysis of the thin film was performed using a scanning electron microscope (SEM) and confirmed that the average crystallite size and thickness of the film were 1.14 μm and 18.65 μm. The principal reflection planes (111), (200), and (220) of the deposited film were identified using X-ray diffractometer (XRD) measurements. Raman microscopy further confirmed the formation of Cu_2O with peaks at 144.4, 525.2, and 620.7 cm^{-1}.

2. INTRODUCTION

Among the numerous metal oxide materials, Copper (I) oxide or cuprous oxide (Cu_2O) is considered a promising material because of its direct band gap $(2.0 - 2.6\ eV)$[1] and high absorption coefficient $(\alpha \sim 10^4 cm^{-1})$[1] in the visible region. In addition, it offers high mobility $(\mu \sim 100\ cm^2/V.s)$[1] and carrier concentration to improve the performance of devices. The material's chemical stability, non-toxicity, and earth abundance are further benefits to be researched for a variety of applications[2].

Cu_2O is natively a p-type semiconductor due to either copper-vacant or oxygen-rich conditions[3]. According to previous studies, ([3]–[7]) n-type conductivity can be obtained by changing the preparation conditions, mainly pH in the solution. A variety of techniques,

including the SILAR technique, Sputtering, Sol-gel, Chemical vapor deposition, Chemical, and Thermal oxidation, etc.[8]–[11] have been used to produce Cu_2O thin films. These techniques all result in p-type Cu_2O thin films. However, these techniques may involve cupric oxide (CuO) impurities and require modern equipment, complex processes, high costs, and temperatures above 100^0C. However, only a few types of research have been published on the production of n-type Cu_2O under specific conditions without the need for external doping. By electrodeposition [4] or by immersing copper electrodes in cupric ions containing aqueous electrolytes [5], [12], n-type Cu_2O thin films can be formed.

In this paper, we present the fabrication process of Cu_2O semiconductor material on ITO glass as well as the structural and morphological properties of the resulting films were investigated in detail using XRD, SEM, and Raman spectroscopy. Additionally, the pH variations of the solution throughout the low temperature thermal oxidation step are also discussed.

3. METHODOLOGY

3.1 Sample Preparation

3.1.1 Electrodeposition Cu Nanoparticles

Copper and ITO conductive glass were used as anode and cathode, respectively. Before the film deposition, both electrodes were cleaned with distilled water and Acetone to remove the impurities. The electrodes were then treated with a 2 $moldm^{-3}$ HCl solution to remove the surface oxidation layers and then dried at room temperature. The electrolyte solution consists of 0.3 $moldm^{-3}$ $CuSO_4$ (40 ml), 0.5 $moldm^{-3}$ H_2SO_4 (40ml), 0.05 $moldm^{-3}$ PEG (Average molecular weight is 400 g/mol^{-1}) (10ml), and 2×10^{-3} $moldm^{-3}$ NaCl (10ml) solutions. The copper electrodeposition was performed at an applied potential of 1V for 20 minutes without stirring the electrolyte solution. The distance between the cathode and anode was kept at 3 cm, and the electrolyte temperature was maintained at room temperature.

3.1.2 Oxidation of Cu Using the Low-Temperature Thermal Oxidation Method

First, the deposited copper films on ITO glass were cleaned with distilled water and Methanol for 10 minutes. Then the substrate was dried using tissue paper and dry air. Then 0.01 $moldm^{-3}$ $CuSO_4$ solution was prepared with the initial pH of the solution being 4.7 at 30℃. Next, the beaker containing the 0.01 $moldm^{-3}$ $CuSO_4$ solutions was placed directly on the hot plate, and the temperature inside the $CuSO_4$ solutions was maintained in between $90 - 95$ ℃. Then, using a sample holder, the deposited copper film on ITO glass was completely immersed in the $CuSO_4$ solution vertically kept for about one hour.

3.2 Thin Film Characterization

The crystalline structure and phase of Cu_2O were determined using an X ray diffractometer (Rigaku Ultima IV) with Cu-Kα radiation, λ=1.5406 A^0, in the 2θ range of $20^0 - 80^0$.The Raman spectra of prepared thin films were investigated using the Raman spectrometer (Thermo Scientific DXR2) with a wavelength of 785 nm and a maximum laser power of 50 mW as an excitation source. Morphological analysis was carried out by the scanning electron microscopy (ZEISS EVO LS15) operated at 10.0 kV.

4. RESULTS AND DISCUSSION

4.1 XRD Analysis

X-ray diffractometer (XRD) measurements were taken in the scan range (2θ) from 20^0 to 80^0 to evaluate the structural properties of the deposited Cu_2O thin films. The XRD pattern of fabricated Cu_2O and electroplated Cu on ITO glass is shown in Figure 1.

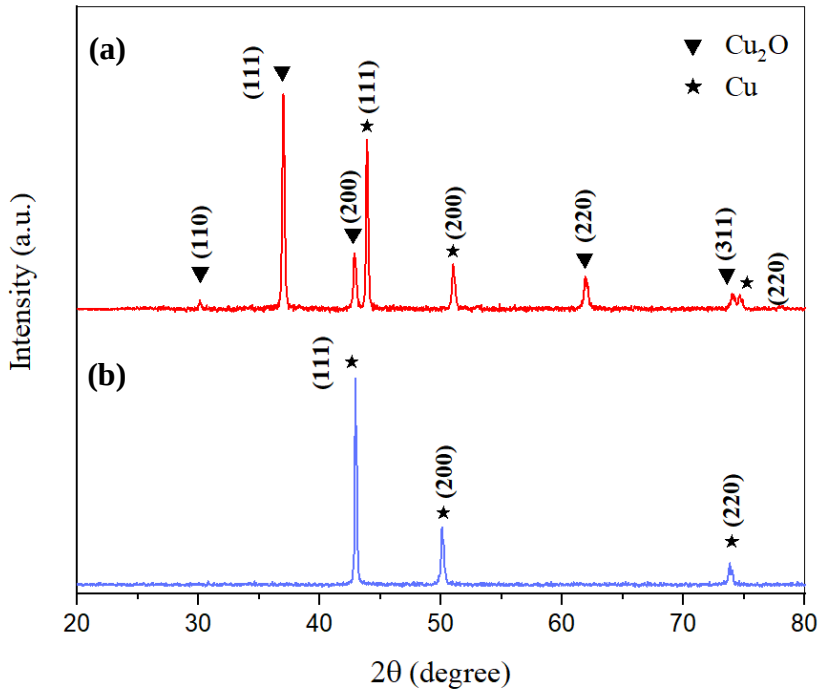

Figure 1: X-ray diffraction (XRD) patterns of (a) Cu_2O thin film and (b) electroplated Cu thin film. However, it has been observed a shift of ~0.6⁰ in each peak of pattern (a) compared to the pattern (b). The reason for this shift is yet to be identified.

XRD pattern (b) show that the Cu peaks only in the deposited copper film on ITO glass at $2\theta = 42.93^0$, 50.10^0, and 73.82^0 are associated with (111), (200), and (220) planes, respectively[13]. These peaks remained in lower intensities in XRD pattern (a) compared to pattern (b) (Table 01) because a few Cu nanoparticles that were not converted into Cu_2O,

were trapped in the Cu_2O thin film. The Cu_2O peaks at $2\theta = 30.11^0$, 36.97^0, 42.86^0, 61.92^0, and 73.97^0 are obtained in XRD pattern (a) corresponds to planes (110), (111), (200), (220), and (311) respectively. However, it has been observed a shift of ~0.6º in each peak of pattern (a) compared to the pattern (b). The reason for this shift is yet to be identified. Therefore, all the Cu_2O peaks and Cu peaks deviated slightly from the literature[14] and that is the reason for the remained Cu peaks in the XRD pattern (a) didn't align with the pattern (b) Cu peaks. But the XRD pattern (b) shows no shift and is consistent with the literature[13]. The cause of the error should be investigated further. However, the sharp XRD peaks at 36.97^0, 42.86^0, and 61.92^0 indicate that the as-prepared Cu_2O thin film has high crystallinity. The purity of the thin film is confirmed as there are no peaks corresponding to Cupric Oxide (CuO) in the XRD pattern (a).

Table 1: The intensity of Cu crystal planes in XRD patterns (a) and (b)

Crystal planes of Cu	Peak intensity at pattern (a) (a.u.)	Peak intensity at pattern (b) (a.u.)
(111)	11605.56	9153.51
(200)	3239.97	2568.11
(220)	1391.16	898.09

4.2 Raman Analysis

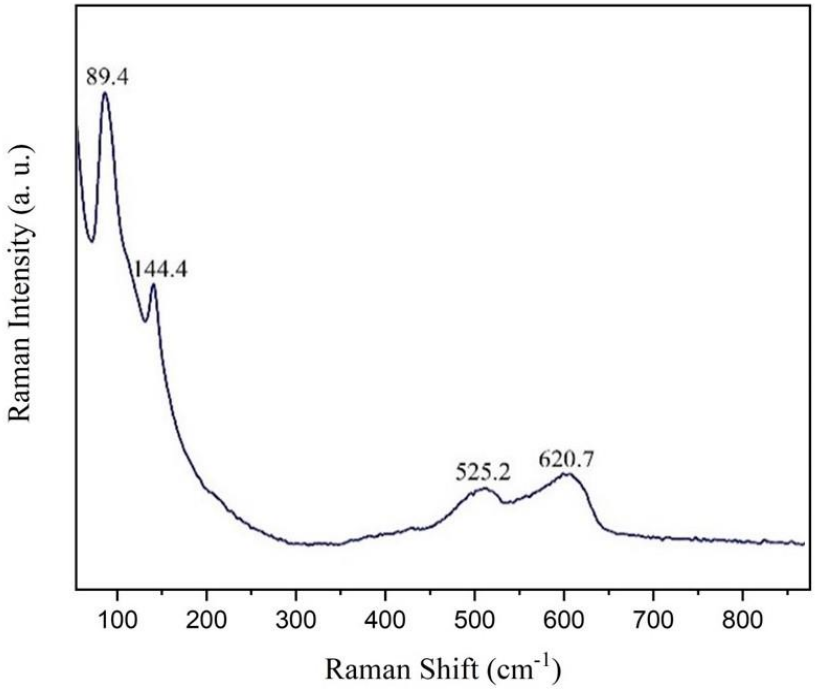

Figure 2:Raman spectra of Cu_2O thin film produced by the low-temperature thermal oxidation. The infrared allowed modes (at 144.4cm^{-1} and 620.7cm^{-1}) and Raman allowed mode (at 525.2cm^{-1}) identified the Cu_2O crystalline structure.

Raman analyses were further used to identify the crystalline structure of the materials. The Raman spectra of deposited Cu_2O thin films are illustrated in Figure 02. The characteristic

phonon frequencies of the crystalline Cu_2O are shown by four Raman peaks observed at 89.4, 144.4, 525.2, and 620.7 cm^{-1}. According to the literature, the infrared allowed mode is associated with the peaks at 144.4 cm^{-1} and 620.7 cm^{-1}[15]. The Raman allowed mode corresponds to the peak at 525.2 cm^{-1}[15]. There is no reference to the corresponding Raman mode for the peak at 89.4 cm^{-1} in the literature. However, the characteristic peaks associated with CuO are expected at 298,330 and 602 cm^{-1} [15], but they could not be detected in this film. Therefore, this method is suitable for producing the pure Cu_2O thin film without any CuO impurities.

4.3 SEM Analysis

The SEM image of electroplated Cu nanoparticles is shown in Figure 03-(a). The Cu nanoparticles have a spherically shaped morphology with considerable aggregation and agglomeration. In order to produce a coating with a spherical form and small particle size, composite additives are added to acidic copper electroplating. This study proves the possibility of producing high performance copper thin films using a PEG-based copper plating solution.

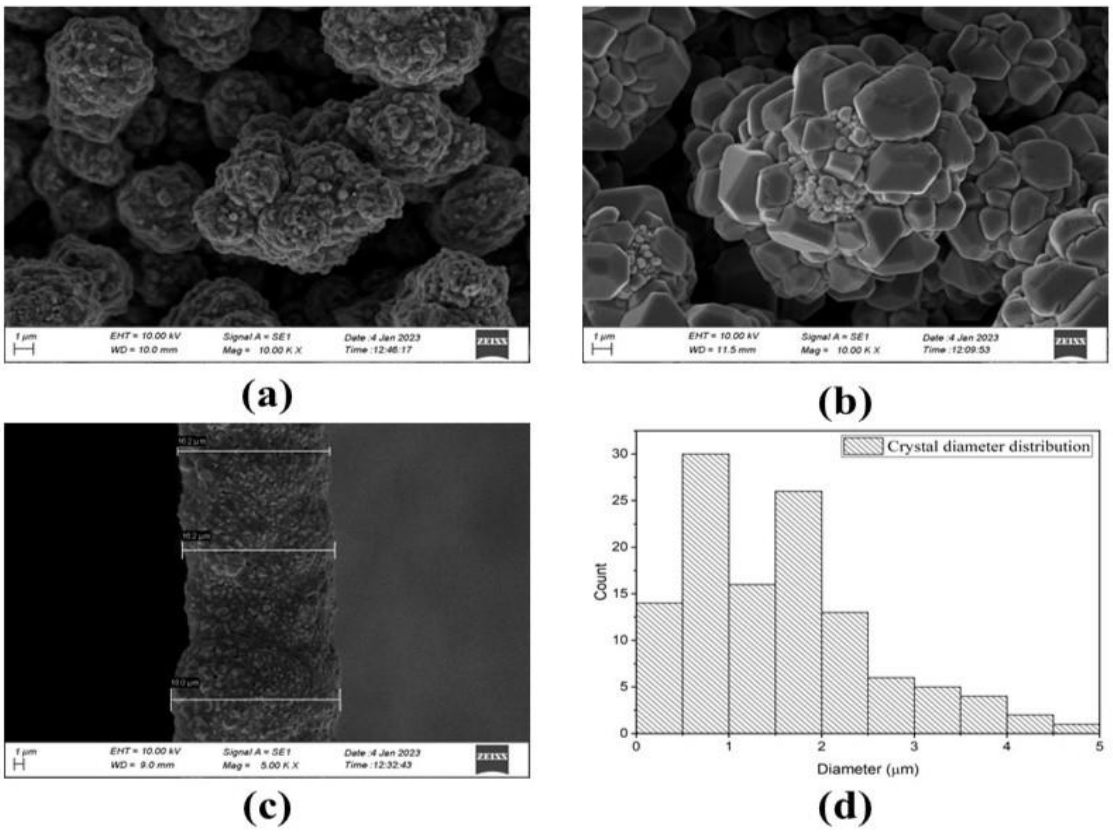

Figure 3: (a) Electroplated Cu nanostructured layer on ITO glass, (b) Cu_2O thin film on ITO glass, (c) Side view of Cu_2O thin film on ITO (gray area), and (d) Distribution plot of Cu_2O crystal diameter.

The SEM image at a magnification of 10k X of the prepared Cu_2O thin film is shown in figure 03-(b). The Cu_2O crystals were only a few micrometers in size and had truncated

octahedral shapes as well as clusters of crystal aggregates on the surfaces. The distribution of crystal diameter was analyzed by size measurements precisely extracted using the ImageJ software in accordance with the scale shown in the SEM image. Hence, the maximum number of particles is in the range of $0.5 - 1.0\ \mu m$, and the average size of the crystal diameter is equal to 1.14 μm. According to figure 03(c), a nearly uniform thickness can be seen. The average thickness of the deposited Cu_2O thin film, as shown in the side view is 18.65 μm.

4.4 pH Observations

In the second step, the pH of the 0.01 $moldm^{-3}$ $CuSO_4$ solution altered over time while producing the Cu_2O films. The pH measurements were taken using a Hach HQ40D portable pH meter during the Cu_2O film formation. Initially, the pH decreased significantly, then the pH reached a stable value, and at that point, the deposition process was stopped to achieve the maximum amount of Cu_2O for the thin film because the formation rate should be equal to the dissolution rate of Cu_2O in an acidic medium.

Table 2: pH variations of 0.01 $moldm^{-3}$ $CuSO_4$ solution during the formation of the Cu_2O thin film at the temperature of 90 to 95 ^0C.

Time (minutes)	pH (In the range of 90-95 ^{0}C)
0	4.24
10	4.14
20	4.09
30	4.03
40	4.00
50	3.98
60	3.98

The preceding explanations allow us to explain step by step the growth mechanism of Cu_2O film formation as follows,

- Step 01, at the Anode,

$$Cu \rightarrow Cu^{2+} + 2e^-$$

At the Cathode,

$$Cu^{2+} + 2e^- \rightarrow Cu$$

- Step 02,

$$Cu^{2+} + Cu \rightarrow 2Cu^+$$

$$2Cu^+ + H_2O \rightarrow Cu_2O + 2H^+$$

As a result, pH decreased when the H^+ ion concentration of the solution is increased as in the equation below,

$$pH = -log_{10}[H^+]$$

5. CONCLUSION

We investigated the fabrication of Cu_2O thin films using the low-temperature thermal oxidation of electrodeposited copper nanoparticles only using $CuSO_4$ solution without any additives. XRD and Raman spectra show the crystal structure and the purity of Cu_2O and the absence of the most probable CuO impurity. SEM image illustrates the crystals of the prepared Cu_2O thin film surface that is in the range of $0.5 - 1.0\ \mu m$, and the thickness of the prepared film is equal to 18.65 μm.

6. ACKNOWLEDGEMENT

The authors wish to convey the sincere thanks to Prof. M M Pathmalal, Department of Zoology, University of Sri Jayewardenepura, for providing the Postgraduate Research Laboratory facilities, and special thanks to Prof. T M W J Bandara, Department of Physics, University of Peradeniya, for opening his Semiconducting Research Laboratory facilities, and providing advance instruments for sample characterization. Also, thanks to Prof. N M S Sirimuthu, Department of Chemistry, University of Sri Jayewardenepura, and Prof. Sanjeewa P K Malvirachchi, Department of Geology, University of Peradeniya, for providing the advanced instrument for the sample characterization of the work. Additionally, the Instrumentation Center of the University of Sri Jayewardenepura is acknowledged for providing advanced instrumentation for sample characterization. Authors also acknowledge the financial assistance from the University of Sri Jayewardenepura Research Council research grant "ASP/01/RE/SCI/2022/37".

7. REFERENCES

[1] O.S. Samuel, A. Olanrewaju, and A. K. David, "*Optical properties of Cu_2O Thin Films Impregnated with Carbon Nanotube (CNT)", Pertanika J. Sci. Technol*., vol. 30, no. 1, pp. 343–350, 2022, doi: 10.47836/pjst.30.1.19.

[2] C. Ravichandiran *et al.*, "*In-depth study on structural, optical, photoluminescence and electrical properties of electrodeposited Cu_2O thin films for optoelectronics: An effect of solution pH," Microelectron. Eng.*, vol. 210, no. March, pp. 27–34, 2019, doi: 10.1016/j.mee.2019.03.013.

[3] K. D. R. N. Kalubowila *et al.*, *" Effect of Bath pH on Electronic and Morphological Properties of Electrodeposited Cu_2O Thin Films ," J. Electrochem. Soc.*, vol. 166, no. 4, pp. D113–D119, 2019, doi: 10.1149/2.0551904jes.

[4] K. M. D. C. Jayathileke, W. Siripala, and J. K. D. S. Jayanetti, *"Electrodeposition of p-type , n-type and p-n Homojunction Cuprous Oxide Thin Films,"* vol. 9, pp. 35–46, 2008.

[5] C. A. N. Fernando, P. H. C. De Silva, S. K. Wethasinha, I. M. Dharmadasa, T. Delsol, and M. C. Simmonds, *"Investigation of n-type Cu_2O layers prepared by a low cost chemical method for use in photo-voltaic thin film solar cells," Renew. Energy*, vol. 26, no. 4, pp. 521–529, 2002, doi: 10.1016/S0960-1481(01)00157-4.

[6] R. P. Wijesundera, M. Hidaka, K. Koga, J.Y. Choi, and N. E. Sung, "*Structural and electronic properties of electrodeposited heterojunction of CuO/Cu_2O,"* no. January, 2010.

[7] K. H. Ã and M. Tao, *"Solar Energy Materials & Solar Cells Electrochemically deposited p – n homojunction cuprous oxide solar cells,"* vol. 93, pp. 153–157, 2009, doi: 10.1016/j.solmat.2008.09.023.

[8] D. S. C. Halin, I. A. Talib, A. R. Daud, and M. A. A. Hamid, *"Characterizations of Cuprous Oxide Thin Films Prepared by Sol-Gel Spin Coating Technique with Different Additives for the Photoelectrochemical Solar Cell,"* vol. 2014, 2014.

[9] A. S. Elmezayyen, S. Guan, F. M. Reicha, I. M. El-sherbiny, and C. Xu, *"Effect of conductive substrate (working electrode) on the morphology of electrodeposited Cu_2O," J. Phys. D. Appl. Phys.*, vol. 175502, p. 175502, doi: 10.1088/0022-3727/48/17/175502.

[10] D. Mohra, M. Benhaliliba, M. Serin, M. R. Khelladi, H. Lahmar, and A. Azizi, *"The investigation of electrodeposited Cu_2O / ITO layers by chronocoulometry process : effect of electrical potential,"* no. May, 2016, doi: 10.1088/1674-4926/37/10/103001.

[11] W. Lee and X. Wang, *"Structural , Optical , and Electrical Properties of Copper Oxide Films Grown by the SILAR Method with Post-Annealing,"* 2021.

[12] I. M. Musa, H. Y. Hafeez, B. I. Adam, I. I. Ibrahim, *"Synthesis with Structural and Morphological Study of n-Cu_2O Layer Produced by Immersion, Boiling and Chemical Bath Heating Techniques of Electroless Deposition Method," Int. J. Sci. Res.*, vol. 6, no. 5, pp. 2478–2484, 2017, [Online]. Available: https://www.ijsr.net/archive/v6i5/ART20162283.pdf.

[13] N. H. Lam *et al.*, *"Evaluation of the Structural Deviation of Cu / Cu_2O Nanocomposite Using the X-ray Diffraction Analysis Methods,"* 2022.

[14] T. Theivasanthi and M. Alagar, *"X-Ray Diffraction Studies of Copper Nanopowder," no. 1.*

[15] D. Cakir, "*Enhanced Raman signatures on copper based-materials*", 2018.